Chinese Physics Letters

LETTER

Emergent Interfacial Magnetism in Epitaxial RuO_2

Cite as: Yudi Yang *et al*. 2026 *Chin. Phys. Lett.* **43** 110801

DOI CSTR

Recommended Articles

Probing the Néel Order in Altermagnetic RuO_2 Films via X-Ray Magnetic Linear Dichroism

Yi-Chi Zhang *et al*.
Chin. Phys. Lett. **42**, 027301 (2025)

All-Altermagnetic Tunnel Junction of RuO_2/NiF_2/RuO_2

Long Zhang, Guangxin Ni, Xuehao Wu, and Guoying Gao
Chin. Phys. Lett. **43**, 040711 (2026)

Magnon Splitting and Magnon Spin Transport in Altermagnets

Kun Wu, Jianting Dong, Meng Zhu, Fanxing Zheng, and Jia Zhang
Chin. Phys. Lett. **42**, 070702 (2025)

ARPES Studies of Spin-Splitting Antiferromagnets

Xinnuo Zhang, Jiayu Liu, Wencheng Huang, Fayuan Zhang, Ming-Yuan Zhu, Yu-Peng Zhu, Chaoyu Chen, Chang Liu, Changyoung Kim, and Dawei Shen
Chin. Phys. Lett. **43**, 050709 (2026)

Circular phonon dichroism in *d*-wave altermagnets

Ding Li, Tao Qin, and Jianhui Zhou
Chin. Phys. Lett. , (2026)

Symmetry-Driven Giant Magneto–Optical Kerr Effects in Altermagnetic Insulator

Jiaxin Luo, Xiaodong Zhou, Jinxuan Liang, Ledong Wang, Qiuyun Zhou, Yong Jiang, Wenhong Wang, Yugui Yao, Luyi Yang, and Wanjun Jiang
Chin. Phys. Lett. **43**, 020713 (2026)

A series journal of Chinese Physical Society distributed by IOP Publishing

Chinese Physics Letters

Chin. Phys. Lett. **43** 110801 (2026)

LETTER

DOI: 10.1088/0256-307X/43/11/110801
CSTR: 32039.14.0256-307X.43.11.110801

Emergent Interfacial Magnetism in Epitaxial RuO_2

Yudi Yang[1,2,3,†], Zhuang Qian[4,†], Shi Liu[2,3,*], and Congjun Wu[3,4,5,*]

[1]Zhejiang University, Hangzhou 310058, China
[2]Department of Physics, Westlake University, Hangzhou 310030, China
[3]Institute of Natural Sciences, Westlake Institute for Advanced Study, Hangzhou 310024, China
[4]Institute for Theoretical Sciences, Westlake Institute for Advanced Study, Westlake University, Hangzhou 310024, China
[5]New Cornerstone Science Laboratory, Department of Physics, Westlake University, Hangzhou 310024, China

[†] These authors contributed equally to this work.
[*]Corresponding authors. Email: liushi@westlake.edu.cn; wucongjun@westlake.edu.cn

The magnetic ground state of the altermagnet candidate RuO_2 remains controversial, with magnetic signatures observed mainly in epitaxial films. Here we show, using first-principles calculations, that magnetism in epitaxial RuO_2 can emerge as an interfacial boundary phase at TiO_2/RuO_2 interfaces. While TiO_2-induced epitaxial strain alone does not make (001)-oriented RuO_2 magnetic, explicit TiO_2/RuO_2 interfaces stabilize sizable Ru moments confined to the first few Ru layers. Charge-density and orbital-resolved analyses reveal interfacial electronic reconstruction, and substrate doping provides a route to tune the induced moments. In symmetric $TiO_2/RuO_2/TiO_2$ heterostructures, the two magnetic interfaces couple through the metallic RuO_2 spacer, producing a thickness-dependent alternation between weak-ferromagnetic and compensated altermagnetic states for even RuO_2 thicknesses. Our results identify interface engineering as a practical route to stabilize and control fragile magnetism in RuO_2.

Altermagnetism combines the zero net magnetization of a compensated antiferromagnet with nonrelativistic momentum-dependent spin splitting, enabling spin-polarized transport without ferromagnetic stray fields [1–4]. In this state, opposite-spin sublattices are related by crystal rotations or mirrors rather than by translation or inversion. Among the earliest and most widely studied candidate altermagnets, metallic rutile RuO_2 has served as a representative platform [5–11]. Yet its intrinsic magnetic ground state remains unsettled. Early neutron and resonant X-ray studies reported compensated magnetic order [12,13], and subsequent thin-film experiments found transport signatures consistent with altermagnetism, including anomalous Hall responses, spin-splitting torques, spin-to-charge conversion, and nonlinear Hall effects [6,8–10,14,15]. In contrast, bulk-sensitive probes, including muon spin rotation, neutron diffraction, and spin-resolved photoemission, have found either no static magnetic order or no clear altermagnetic (AM) spin splitting in high-quality RuO_2 single crystals [16–18].

This experimental dichotomy, recently reviewed by Li *et al.* [19], suggests that magnetic and AM signatures in RuO_2 are strongly sample dependent. They appear mainly in epitaxial films, whereas measurements on pristine bulk crystals increasingly support a nonmagnetic ground state [20]. Additionally, many film-based signatures remain indirect and show appreciable sensitivity to sample quality, suggesting that extrinsic factors such as strain and defects may play an important role [21].

A natural explanation is that RuO_2 lies close to a magnetic instability. Spin-channel Fermi-liquid interactions can dynamically generate unconventional momentum-dependent spin order [22,23], and recent density-functional-theory (DFT) calculations suggest that RuO_2 is near a Landau–Pomeranchuk-type instability [24]. In this near-critical regime, modest changes in hopping amplitudes, induced for example by epitaxial strain, or in Ru-d occupation, modified by charge-carrier doping, can shift the balance among competing magnetic states.

This sensitivity is especially relevant for RuO_2 films grown on rutile TiO_2, whose structural compatibility enables coherent epitaxy along the commonly studied (001), (100), and (110) orientations [6,19]. Recent experiments have further revealed pronounced interfacial polarization in epitaxial RuO_2/TiO_2 heterostructures, highlighting the importance of the local interfacial environment [25]. Because of the anisotropic lattice mismatch, TiO_2-induced strain has been regarded as a key control parameter. However, strain alone cannot fully account for the observations. DFT calculations for strained bulk RuO_2 show that TiO_2-imposed in-plane strain can stabilize magnetic states for the (100) and (110) orientations, but not for the (001)-oriented RuO_2 [26]. This contrasts with the third-order nonlinear Hall response reported in 5-nm (001)-oriented RuO_2 films, which was attributed to intrinsic magnetic order [14]. The discrepancy points to additional interfacial mechanisms beyond purely clamping-induced in-plane strain. Recent theoretical calculations have also reported interface-enhanced magnetism and two-dimensional altermagnetism in RuO_2/TiO_2 superlattices [27].

Here we show that the magnetism of epitaxial RuO_2 is not stabilized by strain alone, but emerges as an interfacial boundary phase driven by TiO_2-induced electronic reconstruction, where the magnetic order is confined to the boundary layers while the bulk-like interior remains essentially nonmagnetic. Direct atomic contact with TiO_2 drives electron transfer into RuO_2; after electronic reconstruction, the added charge is preferentially accommodated by O orbitals, effectively hole-doping the Ru d orbitals and nucleating sizable Ru moments confined to the boundary layers. Additionally, these moments can be enhanced or suppressed by substrate charge doping. In symmetric $TiO_2/RuO_2/TiO_2$ heterostructures, the two magnetic interfaces remain coupled through the metallic RuO_2 spacer, with a thickness-dependent sign change reminiscent of Ruderman–Kittel–Kasuya–Yosida (RKKY) [28–30] exchange. This interfacial coupling enables deterministic selection between a fully compensated AM state and an uncompensated weak-ferromagnetic (WFM) state, establishing a route to the on-demand engineering of fragile magnetism in near-critical RuO_2.

All DFT calculations were performed using Quantum Espresso [31,32] within the Perdew–Burke–Ernzerhof (PBE) form of the generalized-gradient approximation [33] and optimized norm-conserving Vanderbilt pseudopotentials from the PseudoDojo library [34], with a plane-wave cutoff of 80 Ry. The Brillouin zone was sampled using

Received 18 July 2026; accepted 10 October 2026; published 9 November 2026
© 2026 Chinese Physical Society and IOP Publishing Ltd. All rights, including for text and data mining, AI training, and similar technologies, are reserved.

Check for updates

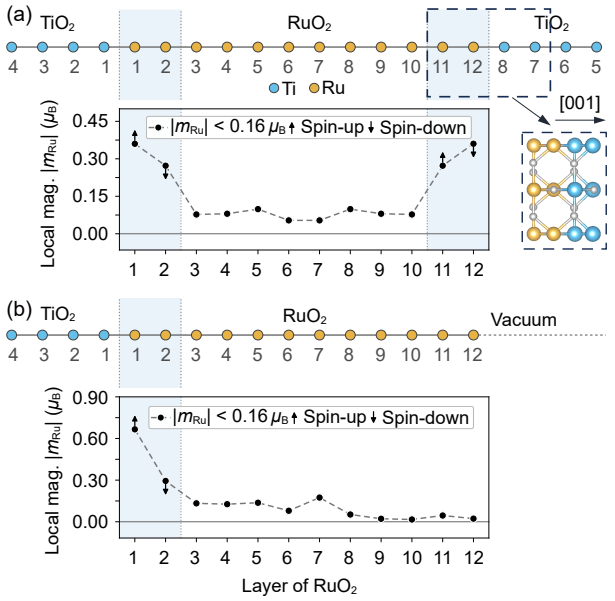

Fig. 1. Layer-resolved local magnetic moments in (001)-oriented RuO_2/TiO_2 heterostructures. (a) Top: schematic structural models, with blue and orange circles denoting Ti and Ru atomic layers, respectively. Bottom: spatial distribution of the absolute Ru local moments, $|m_{Ru}|$, in a heterostructure where 12 Ru atomic layers are sandwiched between TiO_2 layers. The magnetic order is strongly localized in the RuO_2 boundary layers near both interfaces, indicated by the shaded regions, and decays rapidly toward the nonmagnetic interior. Local moments larger than $0.16\mu_B$ are marked by additional arrows indicating their spin orientations. The inset shows a detailed (001) view of the right-hand interface. (b) Corresponding distribution in an asymmetric TiO_2/RuO_2/vacuum slab. The induced moments appear only near the direct TiO_2 contact and are absent at the vacuum-terminated surface.

12×12 and 8×8 in-plane k-point meshes for the primitive and $\sqrt{2}\times\sqrt{2}$ in-plane cells, respectively, together with two out-of-plane k points for periodic sandwich structures and one for slab geometries. We emphasize that no Hubbard U correction was applied to the Ru 4d orbitals.

We first performed DFT calculations for bulk RuO_2 under various epitaxial strain conditions by fixing the in-plane lattice constants and allowing the out-of-plane lattice parameter and internal atomic coordinates to relax. Consistent with previous DFT calculations [26], the in-plane strain imposed by TiO_2 alone is insufficient to make (001)-oriented RuO_2 magnetic [Fig. S1 of the Supplementary Materials (SM)]. We then explicitly constructed TiO_2/RuO_2 heterostructures under periodic boundary conditions, corresponding to TiO_2/RuO_2 superlattices [see the atomic interface structures in Fig. 1(a)]. In these calculations, the in-plane lattice constants of the (001) interface were fixed to those of TiO_2, while the out-of-plane lattice constant and all atomic positions were fully relaxed. Importantly, as shown in Fig. 1(a), Ru atoms near the TiO_2/RuO_2 interfaces develop substantial local magnetic moments exceeding $0.2\mu_B$, and the interfacial moments adopt an uncompensated antiferromagnetic (AFM) ordering. The moments are strongly localized near the interfaces and decay rapidly toward the interior of the RuO_2 slab, where only very small moments remain (below $0.16\mu_B$).

To further isolate the role of the TiO_2 interface, we constructed an asymmetric TiO_2/RuO_2/vacuum slab, in which RuO_2 has one interface with TiO_2 and one bare surface. Because periodic boundary conditions are applied in the in-plane directions, fixing the in-plane lattice vectors to those of TiO_2 ensures that the RuO_2 slab remains under the same epitaxial in-plane strain. As shown in Fig. 1(b), sizable local magnetic moments again appear only in the RuO_2 layers closest to the TiO_2 interface, primarily within the first two Ru layers, and decay quickly away from it. In contrast, the Ru atoms near the vacuum-terminated surface remain essentially nonmagnetic. The absence of surface magnetism demonstrates that the magnetism cannot be attributed to epitaxial strain alone or to generic symmetry breaking. The interfacial electronic reconstruction at the TiO_2/RuO_2 interface is therefore the key ingredient responsible for the emergence of local magnetic moments. These results also show that RuO_2 can become magnetic at the interface in DFT, even without introducing a Hubbard U on the Ru 4d orbitals. We note that additional calculations for the TiO_2/RuO_2 heterostructure with the in-plane lattice constants fixed to the bulk RuO_2 values show the absence of interfacial magnetism, indicating the concerted effect of in-plane strain and interfacial electronic reconstruction.

To analyze charge transfer at the TiO_2/RuO_2 interface, we calculate the planar-averaged differential charge density,

$$\Delta\rho(z) = \rho_{TiO_2/RuO_2}(z) - \rho_{TiO_2}(z) - \rho_{RuO_2}(z), \quad (1)$$

where z is the coordinate normal to the interface, $\rho_{TiO_2/RuO_2}(z)$ is the planar-averaged electronic charge density of the full heterostructure, and $\rho_{TiO_2}(z)$ and $\rho_{RuO_2}(z)$ are those of isolated TiO_2 and RuO_2 slabs evaluated in the same atomic geometry. As shown in Fig. 2(a), sizable charge redistribution is confined to the interfacial atomic layers and decays rapidly away from the interface, closely following the spatial profile of the induced Ru moments. Integrating $\Delta\rho(z)$ over interfacial windows on the TiO_2 and RuO_2 sides yields $\Delta Q_{TiO_2} < 0$ and $\Delta Q_{RuO_2} > 0$ [see Fig. 2(a) inset], indicating net electron transfer from TiO_2 toward interfacial RuO_2. Interestingly, as discussed below, this charge transfer does not amount to simple electron doping of the Ru 4d orbitals.

To identify the orbital character of the electronic reconstruction, we compare the orbital-projected Löwdin occupations of interfacial Ru and O atoms with the averages over the four central RuO_2 layers, which serve as a bulk-like reference. The interfacial Ru atom loses 0.045 e from its 4d manifold, mainly due to a 0.082 e depletion of the d_{xy} orbital, while the other d orbitals show small occupation increases [Fig. 2(b)]. In contrast, the two neighboring O atoms gain 0.085 e in their 2p manifolds, primarily in the p_z orbitals [Fig. 2(c)]. The net charge gain within one interfacial RuO_2 unit is therefore 0.040 e [Fig. 2(d)], consistent with the differential charge density analysis. Thus, although electrons are transferred into the RuO_2 side of the interface, interfacial Ru–O rehybridization redistributes the added charge predominantly toward the O ligand states, leaving the Ru-4d effectively hole doped. This conclusion is further corroborated by the orbital-resolved PDOS analysis presented in the SM, which shows a clear depletion of the occupied interfacial Ru-d_{xy} states.

This reduced Ru-d filling provides a microscopic explanation for the magnetic instability. Previous studies showed that hole doping can induce antiferromagnetism in bulk RuO_2 under suitable tensile strain [24]. More generally, the interfacial electronic reconstruction is intrinsically coupled to the local structural response, as the interface-induced Ru–O distortions modify the crystal-field and hopping environment and thereby affect the orbital hybridization and occupation. The TiO_2/RuO_2 interface realizes this tuning locally: epitaxial tensile strain modifies the Ru–O hopping network, while interfacial orbital rehybridization depletes the Ru-derived states, driving the boundary layers across the near-critical itinerant magnetic instability.

We next performed model calculations to test how interfacial charge transfer affects the induced magnetism. One Ti atom in the central region of the TiO_2 spacer was substituted by p-type Y or n-type Nb. The corresponding dopant concentrations are 5.56% for the odd-layer heterostructures and 6.25% for the even-layer heterostructures, owing to their different TiO_2 stacking configurations as illustrated in Fig. 3(a). Figure 3(b) shows that Y substitution enhances the interfacial Ru moments, whereas Nb substitution suppresses them. The corresponding charge analysis shows that Y reduces, while Nb increases, the net electron accumulation on the RuO_2 side. This trend rules out a simple electron-accumulation mechanism: the larger electron transfer to RuO_2 in the Nb-doped case does not produce larger

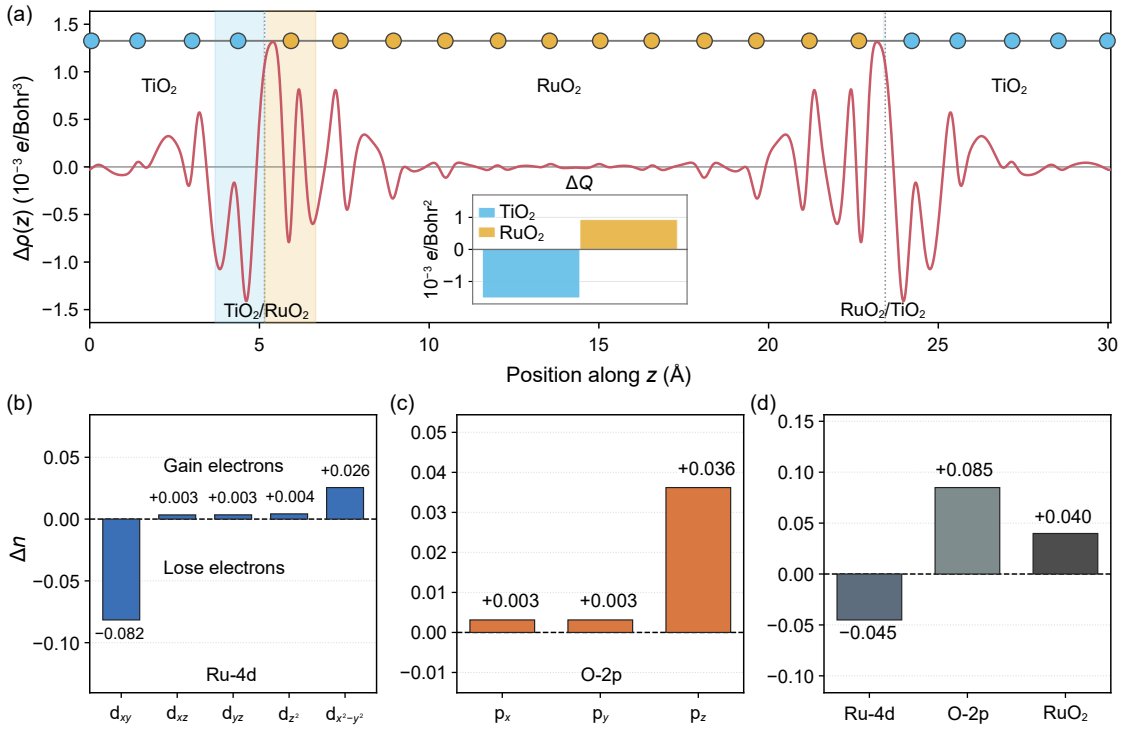

Fig. 2. Interfacial electronic reconstruction in the $TiO_2/RuO_2/TiO_2$ heterostructure. (a) Planar-averaged charge-density difference, $\Delta\rho(z)$, along the out-of-plane direction. The shaded regions denote the TiO_2- and RuO_2-side interface windows used to evaluate the signed integrated charge redistribution, ΔQ, shown in the inset. The integrated charge indicates net electron transfer from TiO_2 to RuO_2 at the interface. (b) and (c) Changes in orbital-projected Löwdin occupations for one interfacial Ru atom and one neighboring O atom, respectively, referenced to the averages over the four central, bulk-like RuO_2 layers. (d) Total occupation changes within one interfacial RuO_2 unit, consisting of one Ru atom and two O atoms. The total is computed in the projected subspace of the Ru-4d and O-2p orbitals. Positive values indicate the gain of electrons.

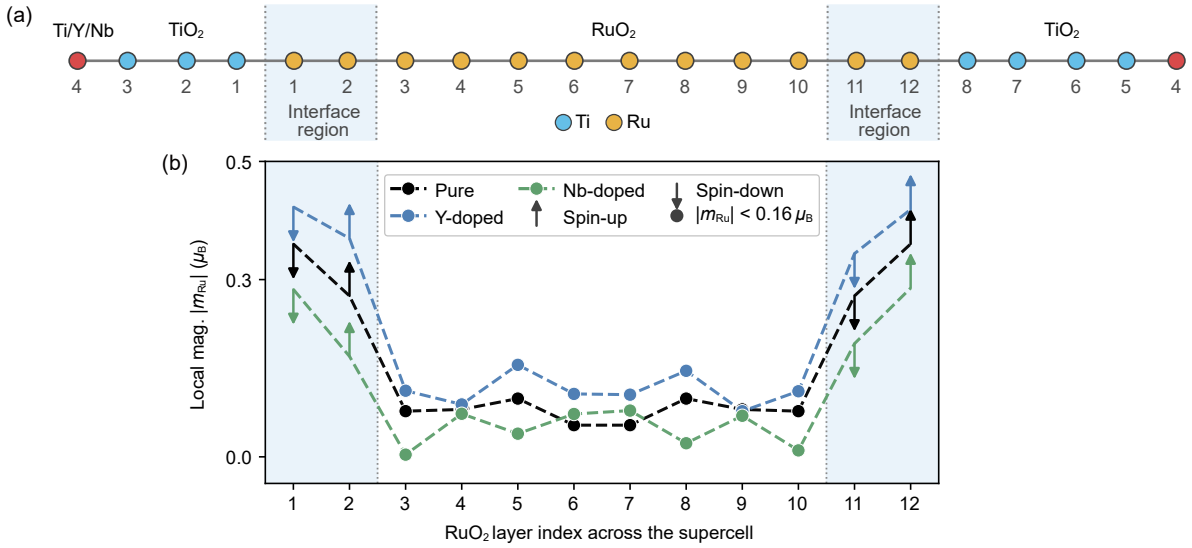

Fig. 3. (a) Schematic of the pristine, Y-doped, and Nb-doped $TiO_2/RuO_2/TiO_2$ heterostructures. (b) Layer-resolved absolute Ru magnetic moments, $|m_{Ru}|$, in pristine, Y-doped, and Nb-doped TiO_2/RuO_2 heterostructures. The p-type Y substitution in the central region of TiO_2 enhances the interfacial Ru moments, whereas n-type Nb substitution suppresses them.

Ru moments. Instead, the result supports an orbital-selective mechanism. Y doping reinforces the depletion of Ru-d states, whereas Nb doping partially compensates it. Thus, the interfacial magnetism is controlled by the Ru-d filling rather than by the total transferred charge. This conclusion is consistent with the hole-enhanced magnetic instability previously identified in strained bulk RuO_2 [24].

As shown in Fig. 1, spin polarization is confined mainly to the two Ru layers closest to each TiO_2/RuO_2 interface. The Ru layer directly adjacent to the interface carries the larger local moment, while the moment in the next Ru layer is smaller and rapidly decays toward the RuO_2 interior. These interfacial Ru moments form an AFM arrangement within each boundary region; however, because the two spin-polarized layers have unequal moment sizes, each interface retains an uncompensated net magnetic moment. This behavior suggests an interesting scenario: in a symmetric $TiO_2/RuO_2/TiO_2$ heterostructure, the two magnetic interfaces may couple through the metallic RuO_2 spacer and align either parallel or antiparallel, as schematically illustrated in Fig. 4. Parallel alignment of the uncompensated interfacial moments produces a finite total magnetization, which we denote as the WFM state [Fig. 4(a)]. In contrast, antiparallel alignment corresponds to an AFM configuration. For an even number of RuO_2

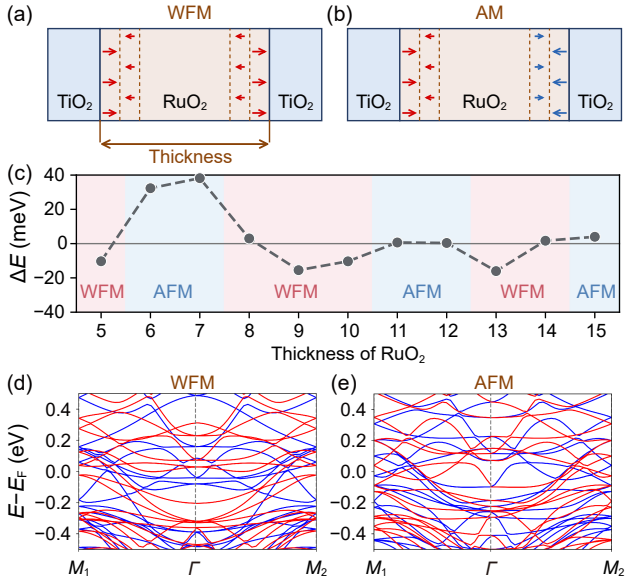

Fig. 4. Interfacial magnetic coupling in $TiO_2/RuO_2/TiO_2$ sandwich structures. (a) Parallel alignment of the interfacial moments produces a WFM state with a finite net magnetization. (b) Antiparallel alignment produces an AFM configuration, which becomes a fully compensated AM state for even RuO_2 thicknesses due to the corresponding crystalline symmetry. (c) Energy difference $\Delta E = E_{\mathrm{WFM}} - E_{\mathrm{AFM}}$ as a function of RuO_2 thickness. Positive values favor the AFM configuration, whereas negative values favor the WFM state. The oscillatory sign change suggests that the metallic RuO_2 interior mediates a relatively long-range, RKKY-like exchange interaction between the magnetic regions localized at the two TiO_2/RuO_2 interfaces. (d) and (e) Spin-resolved band structures of the WFM and AM states, respectively, for a six-layer RuO_2 slab sandwiched between TiO_2 layers.

layers, the relevant spatial symmetry relates the two interfaces and, when combined with spin reversal, enforces a fully compensated AFM state with AM character; we therefore refer to this configuration as the AM state [Fig. 4(b)]. For an odd number of RuO_2 layers, the antiparallel configuration remains AFM but lacks the symmetry required for altermagnetism.

To determine which configuration is favored, we calculate the total-energy difference $\Delta E = E_{\mathrm{WFM}} - E_{\mathrm{AFM}}$, as a function of the RuO_2 thickness. As shown in Fig. 4(c), ΔE exhibits an oscillatory sign change with increasing RuO_2 thickness, indicating that the magnetic ground state alternates between WFM and AFM configurations. The oscillatory sign change with RuO_2 thickness suggests a relatively long-range exchange coupling between the magnetic regions localized at the two TiO_2/RuO_2 interfaces, mediated by the metallic RuO_2 interior and reminiscent of RKKY-like behavior. A definitive identification of the microscopic origin of this coupling, however, will require further dedicated investigation.

We further examined the electronic band structures for the six-layer RuO_2 slab, for which the AFM state is lower in energy than the WFM state. As shown in Fig. 4(d), the WFM state exhibits the conventional spin splitting expected for a ferromagnetic metal. In contrast, the AM state remains metallic and shows momentum-dependent spin splitting characteristic of altermagnetism [Fig. 4(e)], while retaining zero net magnetization. These results show that $TiO_2/RuO_2/TiO_2$ heterostructures provide a tunable platform for engineering magnetic states in RuO_2. By varying the RuO_2 thickness, one can select between WFM, AFM, and AM ground states; by modifying the interfacial charge environment through doping of the TiO_2 layers, one can further tune the induced magnetic moments. Future work could explore how the periodicity of TiO_2/RuO_2 superlattices controls the interfacial coupling and the resulting magnetic phases.

In summary, we have shown that the magnetism observed in epitaxial RuO_2 can be understood as an emergent interfacial boundary phase. While TiO_2-imposed in-plane strain alone does not stabilize magnetism in (001)-oriented RuO_2, explicit TiO_2/RuO_2 interfaces generate sizable Ru local moments confined to the first few boundary layers. The absence of comparable moments at a vacuum-terminated RuO_2 surface, together with the disappearance of interfacial magnetism when the heterostructure is constrained to the bulk RuO_2 in-plane lattice constants, highlights the cooperative role of epitaxial strain and interfacial electronic reconstruction. Charge-density analysis further reveals localized charge redistribution from TiO_2 toward interfacial RuO_2. Importantly, orbital-selective depletion of the Ru-4d states, together with epitaxial strain, plays a key role in stabilizing the local magnetic moments. By tuning the substrate with Y or Nb dopants, the interfacial charge environment and the resulting Ru moments can be systematically modulated. Finally, in symmetric $TiO_2/RuO_2/TiO_2$ heterostructures, the metallic RuO_2 spacer mediates magnetic coupling between the two interfaces, leading to an RKKY-like thickness-dependent alternation between WFM and AFM states, with the even-layer AFM state exhibiting AM character.

These findings establish TiO_2/RuO_2 heterostructures as a tunable platform for controlling fragile magnetism in near-critical itinerant metals. In particular, the RuO_2 thickness provides a direct handle for selecting between uncompensated and compensated magnetic boundary states, while substrate doping offers an additional route to tune the strength of the interfacial moments. More broadly, our results suggest that nonmagnetic oxide boundaries can be used to impose strain as well as to engineer electronic reconstructions to control magnetic order. Future work exploring different interface terminations, dopant distributions, superlattice periodicities, and electrostatic gating could further expand this strategy, enabling on-demand design of AM and WFM phases for spintronic applications.

Acknowledgment

C. W. acknowledges support from the National Natural Science Foundation of China (Grant Nos. 12234016, 12574274, and 12550402), and S. L. from the Zhejiang Provincial Natural Science Foundation of China (Grant No. LR25A040004). This work was supported by the New Cornerstone Science Foundation. Computational resources were supported by the Open Source Supercomputing Center of S-A-I.

References

[1] Šmejkal L, Sinova J, and Jungwirth T 2022 *Phys. Rev. X* **12** 031042
[2] Šmejkal L, Sinova J, and Jungwirth T 2022 *Phys. Rev. X* **12** 040501
[3] Song C, Bai H, Zhou Z, Han L, Reichlova H, Dil J H, Liu J, Chen X, and Pan F 2025 *Nat. Rev. Mater.* **10** 473
[4] Liu Q, Dai X, and Blügel S 2025 *Nat. Phys.* **21** 329
[5] Šmejkal L, González-Hernández R, Jungwirth T, and Sinova J 2020 *Sci. Adv.* **6** eaaz8809
[6] Feng Z, Zhou X, Šmejkal L, Wu L, Zhu Z, Guo H, González-Hernández R, Wang X, Yan H, Qin P, Zhang X, Wu H, Chen H, Meng Z, Liu L, Xia Z, Sinova J, Jungwirth T, and Liu Z 2022 *Nat. Electron.* **5** 735
[7] González-Hernández R, Šmejkal L, Výborný K, Yahagi Y, Sinova J, Jungwirth T, and Železný J 2021 *Phys. Rev. Lett.* **126** 127701
[8] Karube S, Tanaka T, Sugawara D, Kadoguchi N, Kohda M, and Nitta J 2022 *Phys. Rev. Lett.* **129** 137201
[9] Bai H, Han L, Feng X Y, Zhou Y J, Su R X, Wang Q, Liao L Y, Zhu W X, Chen X Z, Pan F, Fan X L, and Song C 2022 *Phys. Rev. Lett.* **128** 197202
[10] Bai H, Zhang Y C, Zhou Y J, Chen P, Wan C H, Han L, Zhu W X, Liang S X, Su Y C, Han X F, Pan F, and Song C 2023 *Phys. Rev. Lett.* **130** 216701
[11] Shao D F, Zhang S H, Li M, Eom C B, and Tsymbal E Y 2021 *Nat. Commun.* **12** 7061
[12] Berlijn T, Snijders P C, Delaire O, Zhou H D, Maier T A, Cao H B, Chi S X, Matsuda M, Wang Y, Koehler M R, Kent P R C, and Weitering H H 2017 *Phys. Rev. Lett.* **118** 077201
[13] Zhu Z H, Strempfer J, Rao R R, Occhialini C A, Pelliciari J, Choi Y, Kawaguchi T, You H, Mitchell J F, Shao-Horn Y, and Comin R 2019 *Phys. Rev. Lett.* **122** 017202

[14] Chu R Y, Han L, Gong Z H, Fu X Z, Bai H, Liang S X, Chen C, Cheong S W, Zhang Y Y, Liu J W, Wang Y Y, Pan F, Lu H Z, and Song C 2025 *Phys. Rev. Lett.* **135** 216703
[15] Jeong S G, Lee S, Lin B *et al*. 2025 *Proc. Natl. Acad. Sci. U.S.A.* **122** e2500831122
[16] Hiraishi M, Okabe H, Koda A, Kadono R, Muroi T, Hirai D, and Hiroi Z 2024 *Phys. Rev. Lett.* **132** 166702
[17] Kessler P, Garcia-Gassull L, Suter A, Prokscha T, Salman Z, Khalyavin D, Manuel P, Orlandi F, Mazin I I, Valenti R, and Moser S 2024 arXiv: 2405.10820 [cond-mat.mtrl-sci]
[18] Liu J, Zhan J, Li T, Liu J, Cheng S, Shi Y, Deng L, Zhang M, Li C, Ding J, Jiang Q, Ye M, Liu Z, Jiang Z, Wang S, Li Q, Xie Y, Wang Y, Qiao S, Wen J, Sun Y, and Shen D 2024 *Phys. Rev. Lett.* **133** 176401
[19] Li Y X, Chen Y, Pan L, Li S, Zhang S B, and Lu H Z 2026 *Sci. China Phys. Mech. Astron.* **69** 257001
[20] Peng X, Liu Z, Zhang S, Zhou Y, Sun Y, Su Y, Wu C, Zhou T, Liu L, Li Y, Wang H, Yang J, Chen B, Li Y, Xi C, Du J, Jiao Z, Wu Q, and Fang M 2025 *Commun. Mater.* **6** 177
[21] Alaei M, Rezaei N, Mikhailov I, Oganov A R, and Qaiumzadeh A 2026 *Commun. Mater.* https://doi.org/10.1038/s43246-026-01292-w
[22] Wu C and Zhang S C 2004 *Phys. Rev. Lett.* **93** 036403
[23] Wu C, Sun K, Fradkin E, and Zhang S C 2007 *Phys. Rev. B* **75** 115103
[24] Qian Z, Yang Y, Liu S, and Wu C 2025 *Phys. Rev. B* **111** 174425
[25] Jeong S G, Lin B Y X, Jin M, Choi I H, Lee S, Yang Z, Nair S, Choudhary R, Parikh J, Santhosh A, Neurock M, Stoerzinger K A, Lee J S, Low T, Tu Q, LeBeau J M, and Jalan B 2026 *Nat. Commun.* **17** 2516
[26] Forte J D S, Jeong S G, Santhosh A, Lee S, Jalan B, and Low T 2025 arXiv:2510.26581 [cond-mat.mtrl-sci]
[27] Xiang Y, Wang Y, Li X, Zhao Z, and Xie W 2026 *J. Phys.: Condens. Matter* **38** 235803
[28] Ruderman M A and Kittel C 1954 *Phys. Rev.* **96** 99
[29] Kasuya T 1956 *Prog. Theor. Phys.* **16** 45
[30] Yosida K 1957 *Phys. Rev.* **106** 893
[31] Giannozzi P, Baroni S, Bonini N *et al*. 2009 *J. Phys. Condens. Matter* **21** 395502
[32] Giannozzi P, Andreussi O, Brumme T *et al*. 2017 *J. Phys. Condens. Matter* **29** 465901
[33] Perdew J P, Burke K, and Ernzerhof M 1996 *Phys. Rev. Lett.* **77** 3865
[34] van Setten M, Giantomassi M, Bousquet E, Verstraete M, Hamann D, Gonze X, and Rignanese G M 2018 *Comput. Phys. Commun.* **226** 39